Experimental study of the human walking-induced fine and ultrafine particle resuspension in a test chamber

Ahmed Benabed, Amir Boulbair, Karim Limam

Experimental study of the human walking-induced fine and ultrafine particle resuspension in a test chamber

Ahmed Benabed[a], Amir Boulbair[a,b], Karim Limam[b]

[a]LaSIE, University of La Rochelle, Av M. Crépeau, 17042 La Rochelle Cedex 01, France

[b]Royal Military Academy RMA, Rue Hobbema 8, 1000 Bruxelles, Belgique

Abstract

In this work, human walking-induced particle resuspension was studied in a full-scale wooden chamber. The mass-based concentrations of PM10, PM2.5, and PM1 and the number-based concentrations of particles sized from 0.01 µm to 1 µm were monitored using a Grimm MiniWRAS counter. Two flooring types were tested: linoleum and hardwood. It has been shown that only mixing with ceiling fan without air supply allows a well-mixed condition to be reached. In this condition and using mass-based and number-based balance equations, emission rates and resuspension fractions were estimated for different particle sizes. The results of the present work show that human walking significantly increases the indoor PM10, PM2.5, and PM1 concentrations. The average estimated PM10, PM2.5, and PM1 resuspension fractions were $(2.1 \pm 0.4) \times 10^{-2}$, $(4.0 \pm 0.7) \times 10^{-3}$ and $(9.0 \pm 0.6) \times 10^{-4}$, respectively for hardwood and $(6.3 \pm 0.6) \times 10^{-3}$, $(8.9 \pm 0.5) \times 10^{-4}$ and $(1.5 \pm 0.3) \times 10^{-4}$, respectively for linoleum. For particles of sizes ranging from 0.01 µm to 1 µm, resuspension fractions increase over several orders of magnitude with increase in particle size for the two floorings. For all particle sizes, the resuspension fractions for hardwood were larger than those for linoleum. No resuspension was recorded for particles smaller than 0.027 µm with linoleum. It has been highlighted in this work that using mass-based concentration underestimates the actual emission proportion of 0.01-0.1 µm particles of the total resuspended particles.

Keywords: Indoor air quality; Particle resuspension; PM (particle matter); Resuspension fraction; Flooring type

1. Introduction

Humans spend most of their time indoors where they may be exposed to potentially harmful pollutants. Some of these indoor pollutants have a negative impact on our comfort, cognitive performance, and health in general [1,2]. Particulate matter (PM) is defined as a complex mixture of microscopic solid or liquid matter suspended in the air. According to their aerodynamic diameter, the particles are classified as fine particles, including PM10 (<10 µm), PM2.5 (<2.5 µm), and PM1 (<1 µm), or ultrafine particles, including PM0.1 (<0.1 µm). It has been shown that in indoor environments, most of the particle mass (82%) is attributable to particles sized from 0.1 to 0.5 µm, whereas most of particles number (73%) are ultrafine particles [3]. Toxicological studies showed that ultrafine particles are associated with a greater inflammatory effect than larger particles [3,4,5,6]. The percentage of respiratory deposition is dominated by the number of sub-0.1 µm particles [4]. It was proposed in [7] that some ultrafine particles provoke both changes in blood coagulability and acute respiratory illness. This hypothesis was based on the number, composition, and size-rather than on the mass-of particles [7].

Particle concentrations in indoor environments can be affected by many factors, including direct emissions from indoor sources, ventilation conditions, the outdoor environment, interior materials and the deposition/resuspension of particles onto/from indoor surfaces [8,9]. It has been shown that human walking-induced particle resuspension is associated with elevated concentrations of inhalable particles in indoor environments [8,10,11]. This phenomenon occurs after an individual's foot impacts a floor that is loaded with particulate matter during walking. Human walking-induced particle resuspension depends on four principal factors: particle properties, floor properties, environmental conditions and walking intensity [11]. In the present work, we will specially focus on the first two factors. Surface properties such as roughness, chemistry, Young's modulus, hygroscopy, and morphology govern the particle-surface interactions and therefore can influence the particle detachment process [12,13]. Ref. [14] showed experimentally that for particles with diameters ranging from 1.0 to 10 µm, carpets are associated with higher particle resuspension rates than vinyl tiles. Ref. [13] showed that particles were more easily detached from hardwood flooring than from linoleum flooring. The authors assumed that there are two main reasons for such behaviour: the difference in the adhesion force (surface energy from the surface materials) and the nature of the micro-roughness of the surfaces. Recently, Ref. [15] showed using a small-scale experiment and an idealized human foot-tapping paradigm that the harder the surface

was, the higher the particle resuspension source strength was. The authors explained this result by stating that mechanical vibrations generated after an individual's foot impacts the floor are amplified with hard surfaces. These vibrations are considered responsible for the particle detachment process that precedes their resuspension.

Table 1 lists some key studies on human walking-induced particle resuspension that studied different flooring types, particle sizes, concentration quantification units, and resuspension coefficients. The table shows that the most commonly used unit in quantifying concentrations in human walking-induced particle resuspension studies is mass/volume. The influence of parameters such as the flooring type and particle size has been widely studied. However, except for the study by Ref. [16], no studies have quantified the resuspension of particles smaller than 0.3 µm. This is due in part to the limitations of the measurement instruments (the lower threshold for most optical particle spectrometers is 0.3 µm) and to the use of mass-based concentrations instead of number-based concentrations to quantify resuspension. This method of quantification does not allow the resuspension of small particles to be quantified because of their small mass.

Table 1. Some key studies on human walking-induced particle resuspension.

Ref	**Flooring**	**Size range**	**Quantification of particle resuspension**	**Resuspension coefficient**
[8]	/	0.3-25 µm	µg/m^3	Resuspension rate coefficient (h^{-1})
[17]	Wood, rug	0.3-2.0 µm	µg/m^3	Resuspension source strength (mg/min)
[18]	Carpet	0.3-2 µm	particles/L	Resuspension rate coefficient (min^{-1})
[19]	Carpet	0.8-10 µm	µg/m^3	Emission factor mg/mg
[16]	Carpet	0.18-18 µm	µg/m^3	Resuspension rate coefficient (h^{-1})
[14]	Carpet, vinyl	0.8-10 µm	particles/m^3	Resuspension rate coefficient (h^{-1})
[20]	Thick carpet	2.7 µm, 7.7 µm	Resuspended mass (g)	Resuspension rate coefficient (s^{-1})
[21]	Paper	PM10	particles/cm^3, µg/m^3	
[22]	Hardwood, vinyl, high-density cut pile carpet, low density cut pile carpet, high-density loop carpet	0.4-10 µm	particles/L	Resuspension fraction
[23]	Vinyl, carpet, wood	PM2.5, PM10	µg/m^3	Resuspension rate coefficient (s^{-1})
[24]	Cotton, denim, polyester	3 µm, 5 µm and 10 µm	µg/m^3	Resuspended mass (µg/m^3)

[25]	Carpet, tile	0.8-10 µm	µg/m^3	Emission rate (mg/h) Resuspension fraction
[15]	Hardwood, vinyl, linoleum, PVC tile, ceramic tile	0.5-10 µm	particles/cm^3	Source strength (particles/s)

Despite the numerous studies that have been carried out to understand human walking-induced particle resuspension, many uncertainties remain, particularly for the resuspension of ultrafine particles. The goal of this work is to study human walking-induced particle resuspension with particles sized 0.01-10 µm in a full-scale test chamber. Particle resuspension was first investigated for PM10, PM2.5, and PM1 and then for particles with diameters ranging from 0.01 µm to 1 µm. The well-mixed condition inside the test chamber was assessed and used to evaluate the particle resuspension fractions and emission rates. The influence of parameters such as the flooring type and particle size on particle resuspension were studied. This work addresses a major knowledge gap for resuspension of particles below 0.3 µm in optical diameter from human walking.

2. Methods and Materials

2.1. Chambers configuration and instrumentation

The experiments were performed in a full-scale wooden chamber (chamber 1 in Figure 1) with a floor area of 2.5 m × 2.5 m and an internal volume of 15.62 m^3. The test chamber was ventilated by an inlet and an outlet of air situated on two opposite walls. The test chamber was also equipped with a three-blade propeller ceiling fan to ensure the indoor air mixing. The ceiling fan rotated with a rotation velocity of 450 rpm. To investigate the influence of flooring type on particle resuspension, two different types of flooring were tested: hardwood and linoleum. The two types of flooring had the same surface areas and covered the entire test chamber floor. Table 2 lists the roughness parameter of the two floorings used during this study (the total height of the profile *Rt*). A two-dimensional analysis using a mechanical tracer stylus was used to estimate this parameter. A second wooden chamber (chamber 2 in Figure 1) with dimensions of 2.5 m × 1.5 m × 2.5 m, in which low concentration levels were maintained (cleaned air was injected during all experiments), was placed in front of the test chamber to prevent test chamber contamination when the door was opened.

Table 2. The total height of the profile of the two floorings.

Flooring	Linoleum	Hardwood
Rt (µm)	27.6	132.10

Alumina powder was used for all the experiments. Alumina or aluminium oxide from ALUMINES DURMAX S.A.R.L located in VIENNE is a chemical component with the molecular formula Al_2O_3 and a density of 3950 kg/m^3. Figures 2(a-b) show the size distribution of the injected polydisperse particles and the fractions of PM10, PM2.5, PM1, PM>10 µm (fractions were calculated with respect to the total mass). The profiles in Figure 2(a) indicate that most of the particles belonged to the smaller particle classes (0.01 µm -0.5 µm). On the other hand, particles with diameters ranging from 0.3 µm to 10 µm dominated the total particle mass. Figure 2(b) shows that more than 92% of the total injected mass of the alumina was PM10 particles. Furthermore, particles larger than 10 µm represented a small fraction of the total mass (7.17%). Particles in this size range are representative, in terms of their diameters, of the particles that are usually encountered inside buildings, which are likely to present a health risk [14]. In this work, the particle sizes are represented as the optical equivalent diameter d_p.

An ejector nozzle from a TOPAS SAG 410 aerosol generator connected to a compressed air source at 200 kPa was used to inject the powder into the test chamber. During the powder injection process, the mechanical interactions between the particles and between the particles and their environments may cause undesirable levels of electrostatic charge. These interactive forces can lead to particle agglomeration or other interactions. In

fundamental aerosol studies, comparable results can only be obtained at controlled and similar charge levels. Thus, an electrostatic aerosol neutralizer, SAG EAN 581, was used to condition the charge distribution of the injected aerosol. The particles were injected into the test chamber by a Bev-line antistatic tube that was 30 cm long and 0.8 cm in diameter, as shown in Figure 1.

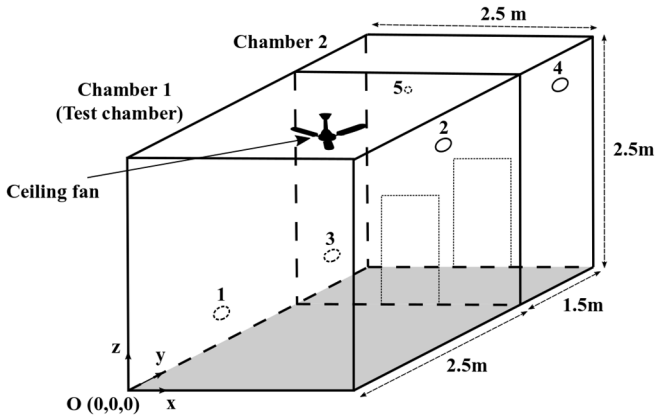

1: Air supply (chamber 1) (x, y, z) = (0, 1.25, 0.35) m 2: Air return (chamber 1) (x, y, z) = (2.5, 1.25, 2.15) m
3: Air supply (chamber 2) (x, y, z) = (0, 3.25, 0.35) m 4: Air return (chamber 2) (x, y, z) = (2.5, 3.25, 2.15) m
5: Powder injection (x, y, z) = (1.25, 2.5, 2.25) m

Figure 1. The geometry of the two chambers and position of air supply, air returned and powder injection orifice.

Temperature and relative humidity were monitored during the experiment using a KIMO KCC 320 sensor.

2.2. Assessment of the well-mixed condition

The experimental procedure commonly used to assess a well-mixed condition in a volume consists of injecting a trace gas, such as sulphur hexafluoride (*SF6*), into the volume and then measuring the gas concentration at different locations in the volume [14]. A well-mixed condition is confirmed once small differences in the concentration between the different locations are recorded. However, this technique remains approximate because unlike gas, the particles forming the aerosol have a certain size distribution and sizes that range several orders of magnitude. The processes of transporting and dispersing particles are strongly associated with the sizes of the particles (e.g., heavy particles cannot consistently follow airflows). In the present work, the well-mixed condition was assessed by the injection of a mass of alumina powder, with m = 0.05 g, inside the test chamber. Concentration monitoring was carried out at three different locations in the chamber by three Grimm optical particle counters (OPC), model 1.108 (see Figure 3). These locations were chosen so that the concentration differences were maximized. The differences in particle concentration at the three locations were measured for different particle sizes. Three cases were tested: (1) supplying air via a vent located in a lateral wall and returning to another vent at the opposite wall with an air change rate of 7.81 m^3/h, as shown in Figure 1, without mixing, (2) same as case 1 with mixing using the ceiling fan, and (3) air mixing using the ceiling fan without air supply.

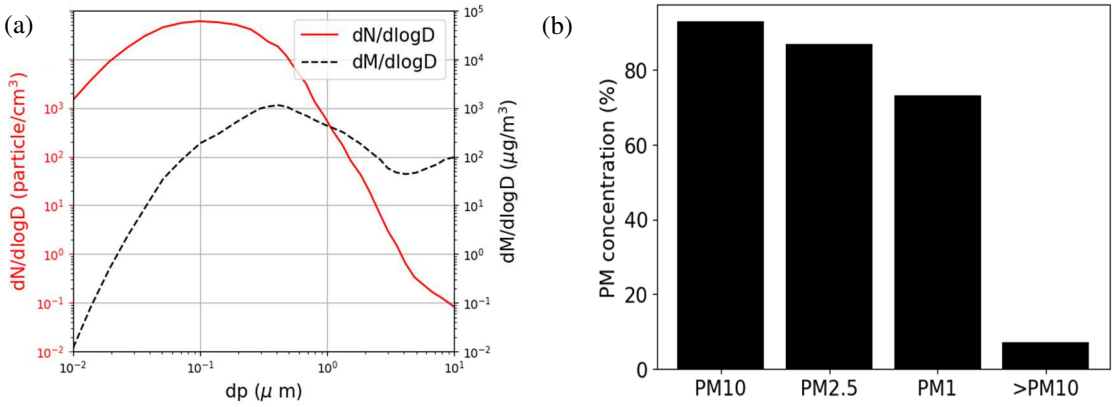

Figure 2. Particle size distribution (a) dN/dlogD and dM/dlogD, (b) fractions with respect to the total mass.

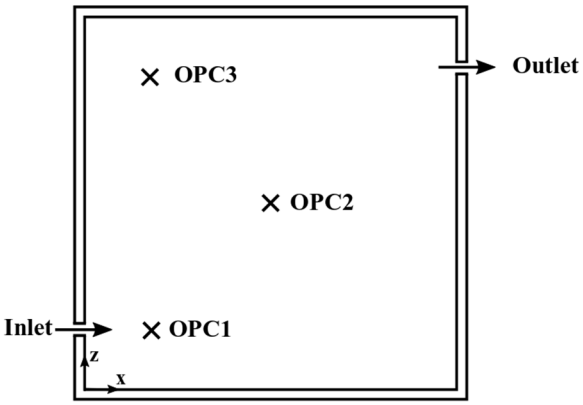

Figure 3. A 2D view of the test chamber showing the locations of the three optical particle counters.

Figures 4(a-f) show the concentration decay over time of 0.4-0.5 µm and 3-4 µm particles concentrations that were recorded at three different locations (see Figure 3) for the three cases. These two sizes were chosen to show the difference in behaviour between small and large particles. The period from when the particles were injected to the time at which the concentration reached a maximum was not plotted; we were interested only in the decay period. Time t = 0 min corresponds to the instant at which the indoor concentration reached a maximum. In the different studied cases, there were no differences in the time to peak concentrations after powder injection. We suppose that, for each measurement point, the time required for the internal concentration to reach the peak after particle injection is relatively short compared to the sampling time.

Figures 4(a-b) represent the concentration variation of the 0.4-0.5 µm and 3-4 µm particles in case 1. Figure 4(a) shows that for the 0.4-0.5 µm particles, there is a small difference between the profiles recorded by OPC2 and OPC3. However, OPC1 shows a different behaviour, with a sharp decrease between t = 0 min and t = 2 min, and a small decrease for t>2 min. The low concentration level recorded by OPC1 is due to the clean air supplied from the vent. Figure 4(b) shows that for the 3-4 µm particles, OPC2 and OPC3 recorded different decay rates, indicating different concentration levels. OPC1 shows similar behaviour as for 0.4-0.5 µm particles with different concentration levels. This difference between concentrations recorded by OPC2 and OPC3 for the 3-4 µm particles (Figure 4(b)) can be explained by the fact that large particles are deposited rapidly under the effect of gravity. This behaviour creates a concentration gradient with a high particle concentration near the floor. However, small particles have relatively low sedimentation velocity and relatively low inertia, and they follow the mixing flow, which explains the similarity between the OPC2 and OPC3 profiles shown in Figure 4(a).

Figures 4(c-d) represent the concentration variation of the 0.4-0.5 µm and 3-4 µm particles in case 2. It can be seen from this figure that the process of mixing the air using the ceiling fan decreased the differences in the concentrations recorded at the three locations compared with case 1. These differences are larger for the 0.4-0.5 µm particles than for the 3-4 µm particles.

Figures 4(e-f) show the evolution over time of the 0.4-0.5 µm and 3-4 µm particles concentrations recorded at three different locations in case 3. It can be seen from the figures that for the two particle sizes, the evolutions of the concentrations inside the chamber at the three measurement locations are identical. This result shows that air mixing with a ceiling fan without air supply ensures a well-mixed condition. In this condition, particle concentration at one location in the volume is representative of the entire volume.

These differences between particle concentrations in a certain configuration indicate that the chamber may not be perfectly mixed during experiments without mixing using the ceiling fan. In this case, some error is introduced by assuming a well-mixed condition. This result also shows that it is difficult to study the influence of the ventilation scheme on particle resuspension. Therefore, the mixing conditions were made consistent for all experiments. In the remainder of this work, the location of OPC2 was chosen to measure particle concentration in the test chamber. There are other ventilation configurations that can be tested and that can provide reasonably well-mixed conditions. However, in this work, we have chosen to test only three configurations because the aim was to highlight the phenomenon and then show that in an extreme case the applicability of the well-mixed condition hypothesis has to be reviewed.

2.3. Particle balance equation

Hereafter, in this paper, the subscript *i* denotes particle size. By assuming no particle coagulation, a well-mixed condition inside the test chamber and a homogenous particle distribution on the flooring surface, for a particle of size *i,* the mass concentration variation inside the test chamber and on the flooring was modelled using the two-compartment balance model, as shown in equations (1.1) and (1.2) [14]:

$$\begin{cases} V\dfrac{dC_{in,i}(t)}{dt} = a_r\, pVC_{out,i}(t) - (a_r + \beta_i)VC_{in,i}(t) + r_{rs,i} f_s A_s L_i(t) + S_i(t) & (1.1) \\ A_r\dfrac{dL_i(t)}{dt} = -r_{rs,i} f_s A_s L_i(t) + \beta_i VC_{in,i}(t) + G_i(t) & (1.2) \end{cases}$$

where

V is the test chamber volume (m^3)

$C_{in,i}$ is the particle concentration inside the test chamber (µg/m^3, or particles/m^3),

$C_{out,i}$ is the particle concentration outside the test chamber (in the chamber 2) (µg/m^3 or particles/m^3),

$r_{rs,i}$ is the resuspension fraction (-),

A_s is the area from which particles are resuspended after the foot-step impact (m^2). It depends on many parameters, such as the walking style, the foot step intensity, and the surface characteristics of the shoe sole. However, this surface is not easy to determine; thus, in this work, we set it equal to the surface area of the sole of the shoe $A_{rs} \approx 0.03$ m^2,

A_r: is the resuspension surface during one-time step (m^2) and it's equal to $n \times A_s$ with n the number of footsteps per time step Δt.

L_i is the floor loading (µg/m^2 or particles/m^2),

a_r is the air exchange rate (h^{-1}),

p is the penetration factor of the test chamber,

S_i is indoor source emission rate (participant's clothes) (µg/h or particles/h).

G_i is the participant's contribution (µg/h or particles/h).

β_i is the deposition rate (h^{-1}),

f_s is the walking rate (steps/h).

The term $r_{rs,i} f_s A_s L_i(t)$ in the equations (1.1) and (1.2) represents the mass or number emission rate for resuspension of particles of size *i* at time *t* (µg/h or particles/h).

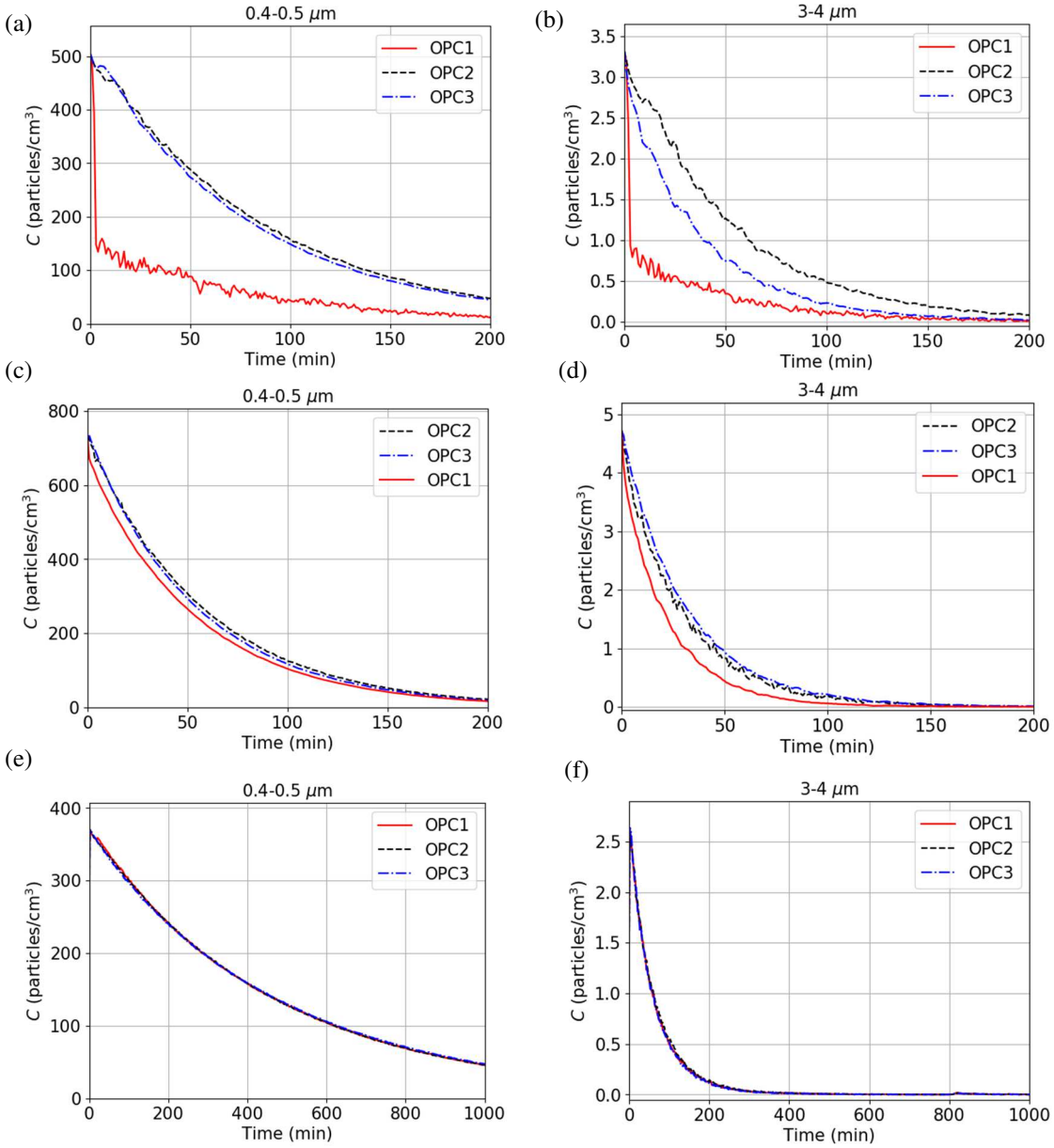

Figure 4. Number concentration (particles/cm^{-3}) versus time for two particle sizes as recorded by three OPC for three ventilation conditions, (a-b) with air supply and without mixing, (c-d) with air supply and with mixing, (e-f) mixing with ceiling fan without air supply.

Knowing that the deposition and natural resuspension of particles (particle resuspension due to the indoor airflow near the surface) cannot easily be evaluated independently, in practice the coefficient β_i used in equations (1.1) and (1.2) considers their global effect. The coefficient $(a_r + \beta_i)$ is called the particle loss rate λ_{loss} of the test chamber. Since the test chamber was isolated from the different sides and was in contact only with chamber 2 with a relatively low particle concentration, the influence of the airborne concentration from outside the test chamber was neglected. Since the participant started the experiences wearing clean coveralls and shoes, and by assuming that the amount of powder collected by the participant during the walking activity was negligible, terms S_i and G_i in equations (1.1) and (1.2) respectively can be neglected. With these assumptions, equations (1.1) and (1.2) become equations (2.1) and (2.2):

$$\begin{cases} V\dfrac{dC_{in,i}(t)}{dt} = -\lambda_{loss,i}VC_{in,i}(t) + r_{rs,i}f_s A_s L_i(t) & (2.1) \\ A_r\dfrac{dL_i(t)}{dt} = -r_{rs,i}f_s A_s L_i(t) + \beta_i VC_{in,i}(t) & (2.2) \end{cases}$$

2.3.1. Loss rate estimation

In the remainder of this work, sampling was carried out by the Grimm particle counter model MiniWRAS. The model combines two measuring instruments: an aerosol spectrometer for particles larger than 0.253 µm and the so-called Nano-sizer for particles smaller than 0.253 µm. This combination of two instruments enables the detection of particles of sizes from 0.01 µm to 35 µm with a sampling time of 1 min. The calibration certificate indicates that the Nanosizer part of the MiniWRAS counter has a 0.35% deviation from a SMPS C. For the OPC part (size greater than 0.253 µm), deviation from the standard is less than 1% for particles of sizes ranging from 0.253 µm to 0.8 µm and less than 8% for particles of sizes ranging from 0.8 µm to 10 µm. These uncertainties were taken into account throughout the study.

Loss rate coefficients in the test chamber were estimated by the following steps prior to the resuspension experiments: the internal surfaces were cleaned, the chamber was closed, the ceiling fan was turned on, and a mass of 0.05 g of alumina powder was injected inside the test chamber. Particle concentration was monitored for 90 min from the moment when the powder was injected. For each studied case, the experiment was repeated 5 times to assess the repeatability of the measurements.

As there were no indoor activity during experiments, the second term of the right-hand side of equation (2.1) was neglected. Equation (2.1) became equation (3):

$$\frac{dC_{in,i}(t)}{dt} = -\lambda_{loss,i}C_{in,i}(t) \qquad (3)$$

The loss rate λ_{loss} was then estimated by an exponential regression of the measured indoor particle concentration *C(t)* (only values obtained with a correlation coefficient higher than 97% were obtained). When the chamber was closed and the ceiling fan turned on, the air change rate a_r was determined to be 0.01 h^{-1} according to the decay of carbon dioxide in the chamber following the removal of the CO_2 source.

2.3.2. Resuspension fraction estimation

In this work, the resuspension fractions were estimated following two steps: (1) seeding and (2) walking.

***Seeding step*:** After the internal surfaces were cleaned, the test chamber was closed and the ceiling fan was turned on, a mass of 12.5 ± 10^{-5} g of alumina powder was injected inside the chamber. The particle counter was not enabled at this stage because high particle concentrations can damage the counter. After 17 h, the time required for the deposition of the majority of the injected aerosol, compressed air at a very low concentration (filtered by a 0.001 µm filter) was injected through the vents of the test chamber for a period of 6 h at a flow rate of 15.62 m^3/h. This step reduces the background noise in the test chamber.

Walking step: After the two particle counters were enabled, a 74 kg, 175 cm male participant entered chamber 2, and donned a previously cleaned coverall and shoes (see Figure 5) and waited 10 min. The participant then entered the test chamber and waited again for 5 min to ensure that any changes in concentration in the test chamber were not due to the opening of the door. The participant walked along the path shown in Figure 6 on the seeded flooring for 10 min with a frequency of 48 steps/min and then sat for 10 min. To accentuate the particle resuspension, the participant deliberately walked in a way such that the heel of his foot was first placed on the floor and then his foot rotated relatively quickly until his toes impact the floor. It is clear that this movement does not correspond to normal human gait; however, it is likely that humans move in this way in some situations, such as during fast walking. In addition, there is no universal way of walking; this process varies across individuals. After 10 min of sitting, the particle counter was stopped. For each studied case, the resuspension experiment was repeated 5 times to assess the repeatability of the measurements. The experiments in the two studied cases were carried out randomly to ensure that any difference between results is only due to the studied parameter (flooring type).

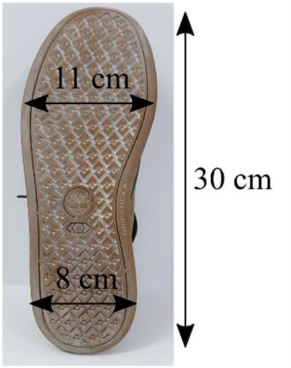

Figure 5. Bottom view of the sole of the shoe used for experiments (42 EU and US).

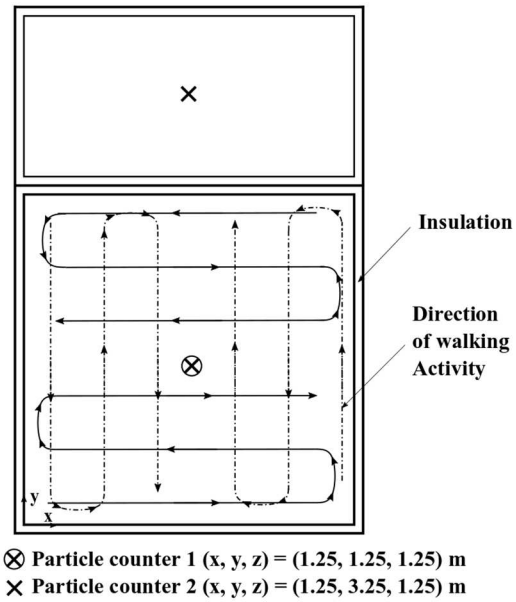

Figure 6. A plan view of the two chambers showing particle counters positions and the direction of walking activity.

It is assumed that the flow generated by the movement of the human does not disturb the flow generated by the fan. Thus, the assumption of a well-mixed volume is maintained. The resuspension fractions were estimated following the approach reported by Ref. [14]. For a particle in size range *i*, the resuspension fraction can be derived from equation (2.1) as shown in equation (4):

$$r_{rs,i}(t) = \frac{V}{f_s A_s L_i(t)} \left(\frac{dC_{in,i}(t)}{dt} + \lambda_{loss,i} C_{in,i}(t) \right) \qquad (4)$$

In equation (4), the continuous indoor particle concentration $C_{in,i}(t)$ is deduced by fitting the measured particle concentration during activity. For this purpose and to have a good adjustment, a 5rd-order polynomial has been used. The continuous floor loading $L_i(t)$ was estimated as follows:

Combining equations (2.1) and (2.2) and rearranging terms, we can write equation (5):

$$A_r \frac{dL_i(t)}{dt} = -V\left(\frac{dC_{in,i}(t)}{dt} + a_r C_{in,i}(t)\right) \quad (5)$$

By integrating both sides of equation (5) from time 0 to t, we can estimate the surface loading $L_i(t)$ at time t by equation (6):

$$L_i(t) = L_i(0) - \frac{V}{f_s A_s}\left(C_{in,i}(t) - C_{in,i}(0) + a_r \int_0^t C_{in,i}(t')dt'\right) \quad (6)$$

Using $L_i(t)$ and $C_{in,i}(t)$, resuspension fraction $r_{rs,i}(t)$ for particle i is determined at each time step using equation (7):

$$r_i(t+\Delta t) = \frac{V}{f_s A_s L_i(t)}\left(\frac{C_{in,i}(t+\Delta t) - C_{in,i}(t)}{\Delta t} + \lambda_{loss,i} C_{in,i}(t)\right) \quad (7)$$

The time step Δt for the approximation is 1 min, which is the same as the Grimm MiniWRAS sampling time. A compound trapezoid formula is used to evaluate the approximate value of the integral $\int_0^t C_{in,i}(t)dt$. Equation (7) can be solved using a numerical forward difference approximation.

2.3.3. Floor loading

The floor loading was estimated following the same resuspension experiments steps without the walking step. This was carried out using a miniature vacuum cleaner, which consists of a fan, an inlet tube with a diameter of 1.1 cm, and a filtration compartment equipped with a HEPA filter with a mass m_0. The vacuum cleaner fan generated an air flow with a rate of 7.5 L/min. Sampling was carried out in four different floor locations, each with an area of 0.25 m^2, to verify the homogeneity of the powder deposition on the floor. The vacuum cleaner was moved through the space several times to ensure that all deposited particles were aspirated. The collected powder and the filter were then weighed using a balance with an accuracy of 10^{-5} g. The mass m of the collected powder was then deduced by subtracting the initial mass of the filter m_0. This step was repeated 3 times to assess the repeatability. The surface concentration was then estimated from the average of the measurements from the different tests. The results of the three tests are shown in Table 3.

Table 3. Averaged mass of the collected powder of the three tests in the two cases. Error bars are standard deviations.

Test	Linoleum	Hardwood
m (g)	0.203 ± 0.018	0.180 ± 0.015

The initial alumina surface loading $L(0)$ values in the two cases as represented in Figure 7 were estimated using the measured powder mass on the different types of flooring shown in Table 3 and using the alumina size distribution. It was assumed that floor loading particle size distributions did not change compared to that of the particles initially injected (see Figure 2(a)).

This study was carried out in two parts. First, resuspension of PM10, PM2.5, and PM1 was studied. In this part, the data given by the particle counter are in µg/m^3. In the second part, we were interested in particles of sizes ranging from 0.01 to 1 µm. In this part, we chose to represent particle concentrations in number/cm^3. During all the experiments, the temperature and RH inside the test chamber were observed to be fairly stable at 23 ± 0.1° C and 35-40 ± 0.1%.

3. Results and discussion

3.1. Resuspension of PM10, PM2.5, and PM1

Figures 8(a-b) show the time variation of PM10, PM2.5 and PM1 mass concentrations for a typical experiment with hardwood inside the two chambers. The times 0 min and 5 min correspond to the instants at which the participant entered the test chamber started the activity, respectively. The profile in Figure 8(a) shows that particle concentration increases sharply after the start of the activity for 3 min then increases slowly until the end of the activity (t = 15 min). The PM10, PM2.5, and PM1 concentration levels reached in the present study

after 2 min of activity are relatively similar to those reported by Ref. [25]. This latter study was carried out in a configuration similar to the configuration of the present study and with 1.5 min of activity. During the experiment, Figure 8(b) indicates that the particle concentration in chamber 2 remained at low levels and that there are no changes in the concentration levels during the experiment.

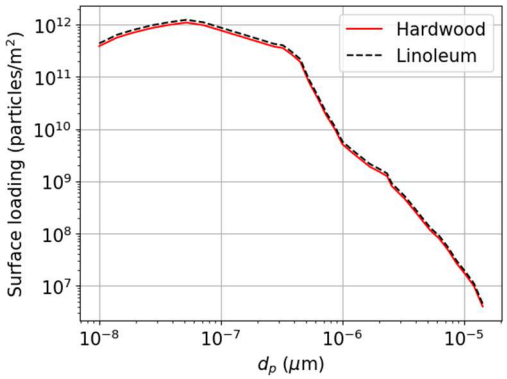

Figure 7. Initial alumina floor loading *L(0)*.

Using equations 3, 6, and 7 and previously obtained values of dust mass loading and air change rates, we determined the PM10, PM2.5, and PM1 loss rate coefficients and resuspension fractions that are presented in Table 4. We can see that the PM10, PM2.5, and PM1 loss rate coefficients for the two cases are similar. This result was expected because the air change rate was constant during the two cases and the only change between the two cases was the type of flooring, which represented 1/6 of the total indoor surfaces. In the present work, for hardwood flooring, the estimated PM10, PM2.5, and PM1 resuspension fractions were 3.3, 4.5, and 6 times greater than those of the linoleum flooring. This result is probably due to the differences between the two materials characteristics which constitute the two floorings [23,15]. Firstly, the hardwood surface roughness parameter *Rt* is 4.8 times larger than that of the linoleum surface (see Table 2). According to Ref. [26], there is an inverse relationship between adhesion force and surface roughness due to the reduction in the contact area between particle and surface. Secondly, the electrostatic charges of surfaces in contact (particle/floor) can also influence particle adhesion. In fact, in our work, despite the neutralization of the particles before being injected into the test chamber, the interactions between the participant's shoes soles and the flooring generate electric charges during walking which get accumulated via the triboelectric effect [27]. These electric charges are higher in the case of linoleum than that of hardwood [28], which leads to a high adhesion force in the case of linoleum flooring.

The PM10 resuspension fraction was 5.2 times and 7.0 times higher than that of PM2.5 with hardwood and linoleum, respectively. The PM2.5 resuspension fraction was 4.4 times and 5.9 times higher than that of PM1 with hardwood and linoleum respectively.

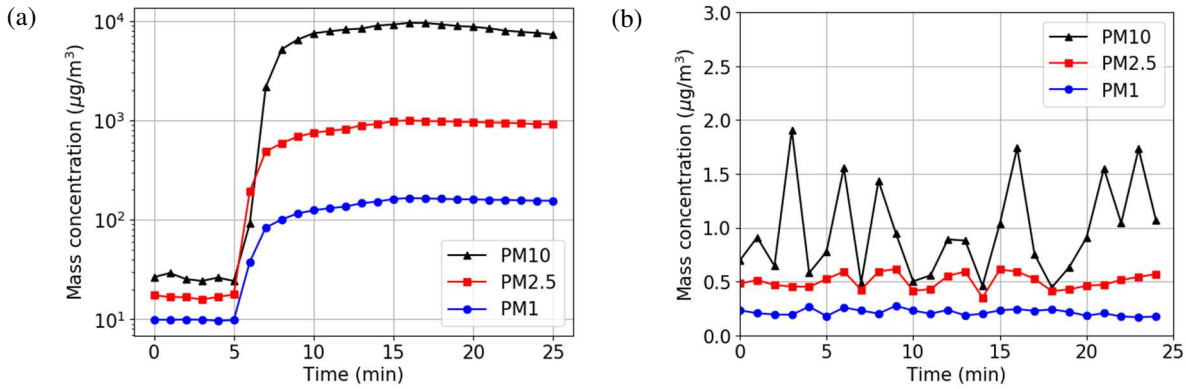

Figure 8. PM10, PM2.5 and PM1 mass concentration versus time measured at fixed locations in (a) chamber 1 and (b) chamber 2.

Table 4. Estimated PM10, PM2.5, and PM1 loss rate and resuspension fractions for the two studied cases. Results are averaged from 5 tests for each case.

	Loss rate coefficients (h^{-1})		Resuspension fractions (-)	
	Linoleum	Hardwood	Linoleum	Hardwood
PM10	$(8.0 \pm 0.7) \times 10^{-1}$	$(6.9 \pm 0.6) \times 10^{-1}$	$(6.3 \pm 0.6) \times 10^{-3}$	$(2.1 \pm 0.4) \times 10^{-2}$
PM2.5	$(2.5 \pm 0.2) \times 10^{-1}$	$(2.3 \pm 0.1) \times 10^{-1}$	$(8.9 \pm 0.5) \times 10^{-4}$	$(4.0 \pm 0.7) \times 10^{-3}$
PM1	$(2.0 \pm 0.3) \times 10^{-1}$	$(1.9 \pm 0.1) \times 10^{-1}$	$(1.5 \pm 0.3) \times 10^{-4}$	$(9.0 \pm 0.6) \times 10^{-4}$

3.2. Resuspension of 0.01-1 µm particles

Figure 9 shows the size-dependent loss rate coefficients of the test chamber for the two studied cases. It can be seen from Figure 9 that there is no significant difference between the two cases. As noted above, this is because the only change between the two cases was the type of flooring, which represented 1/6 of the total indoor surfaces.

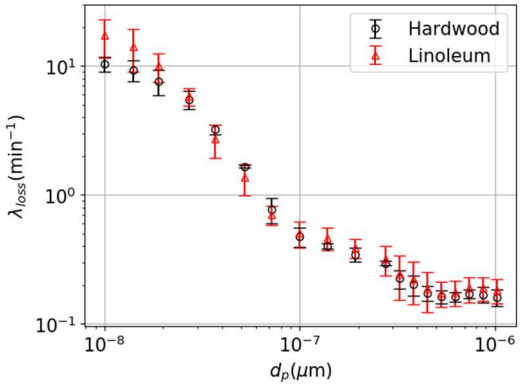

Figure 9. Estimated loss rate coefficients for different sizes for the two studied cases. Loss rates are averaged from 5 tests for each case. Error bars are standard deviations.

Figure 10 represents the number-based concentration (particles/cm^{-3}) versus time for some particles with different sizes, as measured previously, during and after the walking step for one representative experiment at a fixed location inside the test chamber. Times 0 min and 5 min refer to the instant the participant entered the test chamber and the beginning of the activity, respectively. Figure 10 indicates that there were no changes in particle concentration after the participant accessed the test chamber. It can also be seen that 1 min after starting the activity, the particle concentrations of the different sizes increased sharply to 1 order of magnitude higher than the background value, reaching different levels. This observation is in accordance with previous studies in that human walking contributes to a large increase in particle concentrations of different sizes in indoor environments. In addition, the results of the present work indicate that even 0.01-0.3 µm particles are resuspended by human activity. Then, at t = 15 min, the time corresponding to the end of the activity, the concentrations of the different sizes decrease slowly. This decrease is not clearly visible on the curve because the measurement duration after the end of the activity was short.

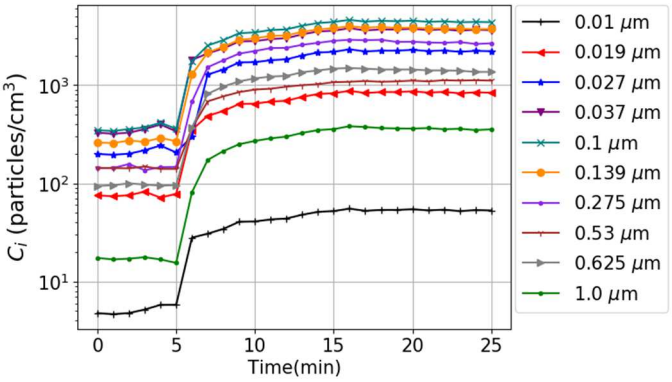

Figure 10. Number concentration (particles/cm^{-3}) versus time for some particles with different sizes measured at a fixed location in the test chamber.

Figure 11 shows the size-dependent resuspension fractions for the two flooring types under similar experimental conditions. In the two studied cases, the particle resuspension fractions increased with increase in particle size. This is due to the adhesion forces of the particles such as the electrostatic force which increases as particle size decreases [29,30]. For hardwood flooring, a sharp increase of particle resuspension fractions as particle size increases was observed between 0.01 µm and 0.027 µm (no particle resuspension was observed for particles smaller than 0.027 µm in the case with linoleum). For both cases, the resuspension fraction increased slowly for particles ranging from 0.027-0.323 µm and then increased sharply for particles ranging from 0.323 µm to 1.0 µm. We also note that the resuspension fractions for hardwood flooring were higher by approximately one order of magnitude than those for linoleum flooring for all particle sizes. As reported before, this difference is due to flooring characteristics. Resuspension fractions of 1 µm particles of the present work are higher than those of Ref. [25]. This is probably due to surface loading determination method, test particles, floorings, experimental conditions, and human activity factors [11].

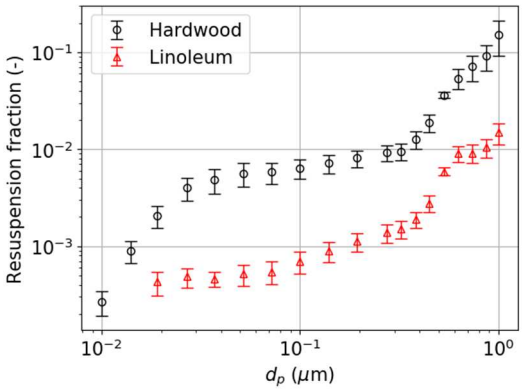

Figure 11. Average resuspension fractions for different sizes for the two floorings. Error bars are standard deviations.

Figure 12 shows the variation in the particle emission rates in µg/h and in particles/h. The variation of the emission rates in the two cases follows particle size distributions (see Figure 2(a)). By comparing the two profiles, we can see that using µg/h as a quantification unit (see Figure 12(a)), emission rate increases with particle size. In addition, there is a large difference between emission rates of large and small particles (seven orders of magnitude). However, using particles/h as a quantification unit (see Figure 12(b)), the profile is quite different, and the difference between sources of different sizes is not large (2.5 orders of magnitude). This result shows that using mass-based concentration underestimates the actual emission proportion of 0.01-0.1 µm particles of the total resuspended particles.

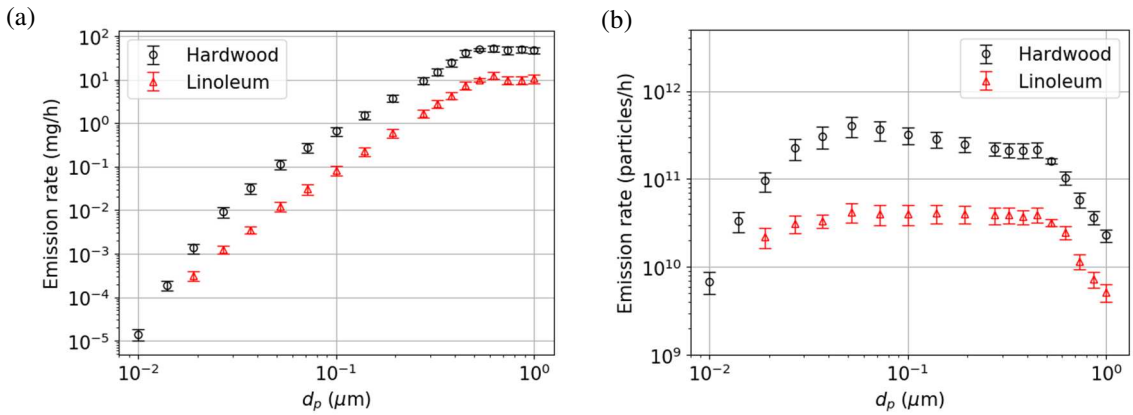

Figure 12. Average emission for different sizes for two floorings averaged from 5 experiments in (a) µg/h and (b) particles/h. Error bars are standard deviations.

4. Conclusion

In this work, human walking-induced particle resuspension in indoor environments was studied experimentally inside a 2.5 m × 2.5 m × 2.5 m wooden chamber. Two flooring types were studied: hardwood and linoleum. Particle concentration was monitored using a Grimm particle counter model MiniWRAS. The resuspension fractions were estimated using particle number/mass balance equations and by assuming a well-mixed condition inside the test chamber. This assumption hypothesis was assessed experimentally by measuring the concentrations of particles of two different sizes at three different locations. It was observed that mixing with a ceiling fan without air supply ensures a well-mixed condition.

This work reveals some important information regarding particle resuspension in indoor environments. First, the resuspension of PM10 is many orders of magnitude higher than those of PM2.5, and PM1. The results also show that human walking can resuspend particles with sizes ranging from 0.01-0.1 µm. This phenomenon is more visible when number-based instead of mass-based quantification is used. For all particle sizes, the particle resuspension values with hardwood flooring were one order of magnitude greater than those with linoleum flooring. In addition, no particle resuspension was recorded for particles of sizes from 0.01-0.027 µm with linoleum.

Investigating other added complications, such as shoe types and walking intensity, can help to better understand human walking-induced particle resuspension. However, these issues remain to be assessed in a future study. Additional investigations using computational fluid dynamics are necessary to better estimate errors caused by the hypothesis of the well-mixing conditions.

Acknowledgments

The authors would like to thank Marc Abadie for his helpful advice and comments.

References

[1] M.J. Mendell, Indoor residential chemical emissions as risk factors for respiratory and allergic effects in children: A review, Indoor Air. 17 (2007) 259–277. https://doi.org/10.1111/j.1600-0668.2007.00478.x.

[2] N.E. Klepeis, W.C. Nelson, W.R. Ott, J.P. Robinson, A.M. Tsang, P. Switzer, J. V. Behar, S.C. Hern, W.H. Engelmann, The National Human Activity Pattern Survey (NHAPS): A resource for assessing exposure to environmental pollutants, J. Expo. Anal. Environ. Epidemiol. 11 (2001) 231–252. https://doi.org/10.1038/sj.jea.7500165.

[3] A. Peters, H.E. Wichmann, T. Tuch, J. Heinrich, J. Heyder, Respiratory effects are associated with the number of ultrafine particles, Am. J. Respir. Crit. Care Med. 155 (1997) 1376–1383. https://doi.org/10.1164/ajrccm.155.4.9105082.

[4] A.P. Shah, A.P. Pietropaoli, L.M. Frasier, D.M. Speers, D.C. Chalupa, J.M. Delehanty, L. Huang, M.J. Utell, and M.W Frampton, Effect of inhaled carbon ultrafine particles on reactive hyperemia in healthy human subjects, Environ. Health Perspect. 116 (2008) 375–380. https://doi.org/10.1017/CBO9781107415324.004.

[5] J. Ferin, Pulmonary retention and clearance of particles, Toxicol. Lett. 72 (1994) 121–125. https://doi.org/10.1016/0378-4274(94)90018-3.

[6] G. Oberdorster, J. Ferin, R. Gelein, S.C. Soderholm, J. Finkelstein, Role of the alveolar macrophage in lung injury: Studies with ultrafine particles, Environ. Health Perspect. 97 (1992) 193–199. https://doi.org/10.2307/3431353.

[7] A. Seaton, D. Godden, W. MacNee, K. Donaldson, Particulate air pollution and acute health effects, Lancet. 345 (1995) 176–178. https://doi.org/10.1016/S0140-6736(95)90173-6.

[8] T.L. Thatcher, D.W. Layton, Deposition, resuspension, and penetration of particles within a residence, Atmos. Environ. 29 (1995) 1487–1497. https://doi.org/10.1016/1352-2310(95)00016-R.

[9] G.C. Morrison, W.W. Nazaroff, J.A. Cano-Ruiz, A.T. Hodgson, M.P. Modera, Indoor air quality impacts of ventilation ducts: Ozone removal and emissions of volatile organic compounds, J. Air Waste Manag. Assoc. 48 (1998) 941–952. https://doi.org/10.1080/10473289.1998.10463740.

[10] I. Goldasteh, Y. Tian, G. Ahmadi, A. R. Ferro, Human induced flow field and resultant particle resuspension and transport during gait cycle, Build. Environ. 77 (2014) 101–109. https://doi.org/10.1016/j.buildenv.2014.03.016.

[11] J. Qian, J. Peccia, A.R. Ferro, Walking-induced particle resuspension in indoor environments: A review, Indoor Air 2014 - 13th Int. Conf. Indoor Air Qual. Clim. (2014) 366–368.

[12] C. Henry, J.P. Minier, Progress in particle resuspension from rough surfaces by turbulent flows, Prog. Energy Combust. Sci. 45 (2014) 1–53. https://doi.org/10.1016/j.pecs.2014.06.001.

[13] I. Goldasteh, G. Ahmadi, A.R. Ferro, Wind tunnel study and numerical simulation of dust particle resuspension from indoor surfaces in turbulent flows, J. Adhes. Sci. Technol. 27 (2013) 1563–1579. https://doi.org/10.1080/01694243.2012.747729.

[14] J. Qian, A.R. Ferro, Resuspension of dust particles in a chamber and associated environmental factors, Aerosol Sci. Technol. 42 (2008) 566–578. https://doi.org/10.1080/02786820802220274.

[15] A. Benabed, K. Limam, B. Janssens, W. Bosschaerts, Human foot tapping-induced particle resuspension in indoor environments: Flooring hardness effect, Indoor Built Environ. (2019). https://doi.org/10.1177/1420326X19856054.

[16] J. Qian, A.R. Ferro, K.R. Fowler, Estimating the resuspension rate and residence time of indoor particles, J. Air Waste Manag. Assoc. 58 (2008) 502–516. https://doi.org/10.3155/1047-3289.58.4.502.

[17] A.R. Ferro, R.J. Kopperud, L.M. Hildemann, Source Strengths for Indoor Human Activities that Resuspend Particulate Matter, Environ. Sci. Technol. 38 (2004) 1759–1764. https://doi.org/10.1021/es0263893.

[18] C. Gomes, J. Freihaut, W. Bahnfleth, Resuspension of allergen-containing particles under mechanical and aerodynamic disturbances from human walking, Atmos. Environ. 41 (2007) 5257–5270. https://doi.org/10.1016/j.atmosenv.2006.07.061.

[19] J.A. Rosati, J. Thornburg, C. Rodes, Resuspension of particulate matter from carpet due to human activity, Aerosol Sci. Technol. 42 (2008) 472–482. https://doi.org/10.1080/02786820802187069.

[20] and C.E.R. R.C. Oberoi, J.I. Choi, J.R. Edwards, J.A. Rosati, J. Thornburg, Human-induced particle re-suspension in a room, Aerosol Sci. Technol. (2010).

[21] N. Serfozo, S.E. Chatoutsidou, M. Lazaridis, The effect of particle resuspension during walking activity to PM10 mass and number concentrations in an indoor microenvironment, Build. Environ. 82 (2014) 180–189. https://doi.org/10.1016/j.buildenv.2014.08.017.

[22] Y. Tian, K. Sul, J. Qian, S. Mondal, A.R. Ferro, A comparative study of walking-induced dust resuspension using a consistent test mechanism, Indoor Air. 24 (2014) 592–603.

https://doi.org/10.1111/ina.12107.

[23] S. You, M.P. Wan, Experimental investigation and modelling of human-walking-induced particle resuspension, Indoor Built Environ. 24 (2015) 564–576. https://doi.org/10.1177/1420326X14526424.

[24] A. McDonagh, M.A. Byrne, The influence of human physical activity and contaminated clothing type on particle resuspension, J. Environ. Radioact. 127 (2014) 119–126. https://doi.org/10.1016/j.jenvrad.2013.10.012.

[25] A.C.K. Lai, Y. Tian, J.Y.L. Tsoi, A.R. Ferro, Experimental study of the effect of shoes on particle resuspension from indoor flooring materials, Build. Environ. 118 (2017) 251–258. https://doi.org/10.1016/j.buildenv.2017.02.024.

[26] C.L.C. Tan, S. Gao, B.S. Wee, A. Asa-Awuku, B.J.R. Thio, Adhesion of dust particles to common indoor surfaces in an air-conditioned environment, Aerosol Sci. Technol. 48 (2014) 541–551. https://doi.org/10.1080/02786826.2014.898835.

[27] L.A. Kessler, W.K. Fisher, A study of the electrostatic behavior of carpets containing conductive yarns, J. Electrostat. 39 (1997) 253–275. https://doi.org/10.1016/S0304-3886(97)81203-X.

[28] D.M. Gooding, G.K. Kaufman, Tribocharging and the Triboelectric Series, Encycl. Inorg. Bioinorg. Chem. (2019) 1–14. https://doi.org/10.1002/9781119951438.eibc2239.pub2.

[29] J.Q. Feng, D.A. Hays, Relative importance of electrostatic forces on powder particles, Powder Technol. 135–136 (2003) 65–75. https://doi.org/10.1016/j.powtec.2003.08.005.

[30] O.R. Walton, Review of adhesion fundamentals for micron-scale particles, KONA Powder Part. J. 26 (2008) 129–141. https://doi.org/10.14356/kona.2008012.